Materials Letters 302 (2021) 130340

Contents lists available at ScienceDirect

Materials Letters

journal homepage: www.elsevier.com/locate/matlet

Carrier-free resveratrol nanoparticles: Formulation development, *In-vitro* anticancer activity, and oral bioavailability evaluation

Ashok Kumar Jangid [a], Krunal Patel [b], Poonam Jain [a], Sunita Patel [b], Kanakaraju Medicherla [c], Deep Pooja [d,*], Hitesh Kulhari [a,*]

[a] School of Nano Sciences, Central University of Gujarat, Gandhinagar 382030, Gujarat, India
[b] School of Life Sciences, Central University of Gujarat, Gandhinagar 382030, Gujarat, India
[c] Department of Human Genetics, College of Science and Technology, Andhra University, Visakhapatnam 530003, Andhra Pradesh, India
[d] The Centre for Advanced Materials & Industrial Chemistry, School of Sciences, RMIT University, Melbourne 3000, Australia

ARTICLE INFO

Keywords:
Resveratrol
Nanoparticle
Human colorectal cancer
Bioavailability

ABSTRACT

Resveratrol nanoparticles (RNP) formulation was prepared with 0.5% w/v of SDS and confirmed by TEM, XRD, DSC, XRD, FTIR and NMR. The prepared RNP were evaluated for physicochemical properties like solubility, stability, dissolution profile and partition coefficient. The anticancer activity of prepared RNP formulation was determined against HCT 116 human colorectal cancer cells by cell viability and apoptosis studies. An *in vivo* pharmacokinetic study in SD rats showed that, the AUC of the RNP was significantly higher ($p < 0.0001$) than the pure RSV. The plasma C_{max} was found to be 0.23 ± 0.02 μg/mL for RSV and 0.62 ± 0.09 μg/mL for RNP. An increase in AUC and C_{max} suggested that, the developed formulation was more bioavailable than the pure RSV.

1. Introduction

Solubility is the major hurdle for many potential bioflavonoids and synthetic drugs and creates hurdles in their product development and commercialization [1]. Various bioflavonoids suffer from less water solubility and poor bioavailability due to their weakly acidic or weakly basic nature [2]. These molecules produce several important health benefits, but the therapeutic efficacies of these molecules are limited due to their poor physicochemical properties and hence unfavourable pharmacokinetic (PK) profiles after administration. Among the various type of nanocarriers, the preparation of drug nanoparticles (DNPs) using a size reduction technique looks like a better approach, particularly when the solubility and bioavailability enhancement are primary objectives [3]. Further, a significant decrease in the crystallinity of drugs is observed during the preparation of DNPs, which also helps to improve the physicochemical properties of drugs [4].

Resveratrol (RSV) is a naturally occurring, BCS-II polyphenolic compound and prominently found in grapes, dark berries, red wine or peanuts etc [5]. The RSV is well reported to show the potential therapeutic benefits [6] however, it has poor water solubility (30 μg/mL) and low oral bioavailability with a partition coefficient of 3.1 which limits its pharmacological activities [7]. Therefore, we have prepared carrier-free, amorphous RSV nanoparticles (RNP) formulation for the enhancement of solubility, dissolution and oral bioavailability of RSV. The prepared RNP was explored by TEM, XRD, DSC, FTIR and NMR. Then, in-vitro dissolution, cytotoxicity and pharmacokinetic studies were investigated.

2. Experimental section

The carrier-free RNP were prepared by the ultra-nanoprecipitation method. All these experimental details can be found in Supplementary Material.

3. Results and discussion

3.1. Preparation and characterization of resveratrol nanoparticle (RNP)

Tables S1 and S2 show the particle size, polydispersity index and zeta potential of RNP with 0.5% w/v of SDS showing the particle size (76 nm), monodispersity (PDI ~ 0.212) and good zeta potential (-18 mV). Fig. 1**a-c** shows the TEM image and Selected Area Electron Diffraction (SAED) pattern of the final optimized RNP formulation. The suspended RNP particles were almost spherical and well dispersed with a particle

* Corresponding authors.
E-mail addresses: d.dpooja00@gmail.com (D. Pooja), hitesh.kulhari@cug.ac.in (H. Kulhari).

https://doi.org/10.1016/j.matlet.2021.130340
Received 11 March 2021; Received in revised form 13 June 2021; Accepted 23 June 2021
Available online 28 June 2021

size ~ 8 nm Fig. 1**b** illustrates the SAED pattern of prepared RNP where no diffraction spots were observed, suggesting the amorphous nature of the RNP. Fig. 1**d** represents the PXRD patterns of RSV and RNP formulation where RSV showing the peaks at 2θ angles 6.7°, 13.2°, 16.4°, 19.1°, 22.2°, 23.5°, 25.3°, 28.4°, 31.6°, 33.0°, 33.8° and 38.4° which suggested the crystalline nature of RSV [8]. Interestingly, the diffraction peaks of RSV were not observed in RNP spectra which indicated the amorphous nature of the formulation. Fig. 1**e** depicts the DSC thermogram, which showed a sharp endothermic peak at 263 °C. The DSC thermogram of RNP shows the two different endothermic peaks at 246 and 235 °C but with peak shifting. The shifting of the sharp endothermic peak of RSV further confirmed the change in the physical nature of the RNP. Fig. 1**f** showed the FTIR spectra of RNP which shows the peaks at 3268 cm^{-1} (O–H stretching), 1608 (C = C stretching of aromatic ring), 1585 and 1465 cm^{-1} (C = C trans double bond stretching), 1390 cm^{-1} (C-O-C stretching), 1155 cm^{-1} (phenolic C-O stretching), 962 cm^{-1} (trans C = C stretching), 833 cm^{-1} (=C–H vibration bands of phenolic ring), 616–517 cm^{-1} (=C–H vibration bands of trans double bond). [9]. Fig. 1**g** shows the ^{1}H NMR spectra of RSV, SDS, physical mixture (RSV + SDS 1:1 w/w), and RNP. The FTIR and ^{1}H NMR spectra of RNP showed all protons like pure RSV with a very slight shift confirming the removal of SDS and no change in RSV after formulating as drug nanoparticles.

3.2. Physicochemical properties of resveratrol nanoparticles (RNP)

Solubility and partition coefficient (log P) of RSV and RNP are shown in Fig. 2**a-b**. The solubility of RSV in water was 36.6 ± 1.92 μg/mL with Log P value of 3 whereas RNP had the solubility of about 321.43 ± 7.07 μg/mL with 2.5 Log P value. From the observed solubility data, it was observed that the solubility of RSV was significantly (8.7 times, $p < 0.0001$) increased with decreasing Log P value after nanoparticle formation. The reduction in particles and the amorphous nature of the RNP might be responsible for solubility enhancement and a decrease in the Log P value of RSV [10]. The dissolution profile was higher for RNP than the pure RSV in both the media. After 2 h, dissolution of RSV and RNP in 0.1 N HCl was found to be 11.4% and 51.3%, respectively. In phosphate buffer pH 6.8, dissolution of RSV and RNP was 30.4% and 91.01%, respectively after 30 min (Fig. 2**c-d**) which may be due to reduction in particle size, decrease in hydrophobicity and amorphous nature of RNP [10]. Table S3 shows the change in physicochemical properties of the RNP formulation after three months of storage. No significant changes were observed in particle size, PDI and zeta potential of RNP. The

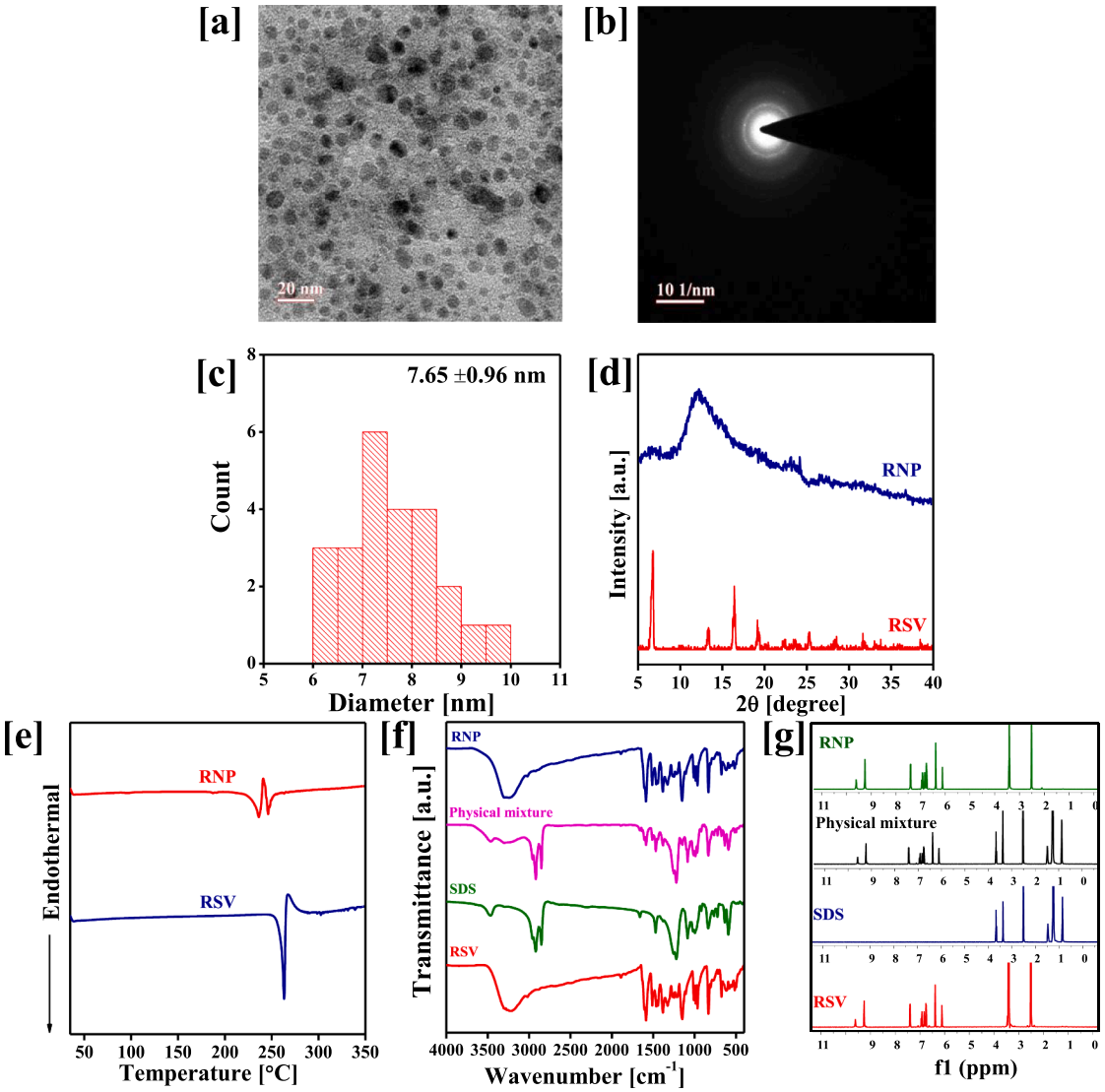

Fig. 1. Characterization: (a) TEM image of RNP, (b) SAED pattern of RNP, (c) Size distribution of RNP, (d) PXRD patterns of RSV and RNP (e) DSC scans of RSV and RNP, (f) FTIR spectra of RSV, sodium dodecyl sulphate (SDS), physical mixture (RSV + SDS 1:1 w/w) and RNP and (g) ^{1}H NMR spectra RSV, SDS, RSV + SDS and RNP.

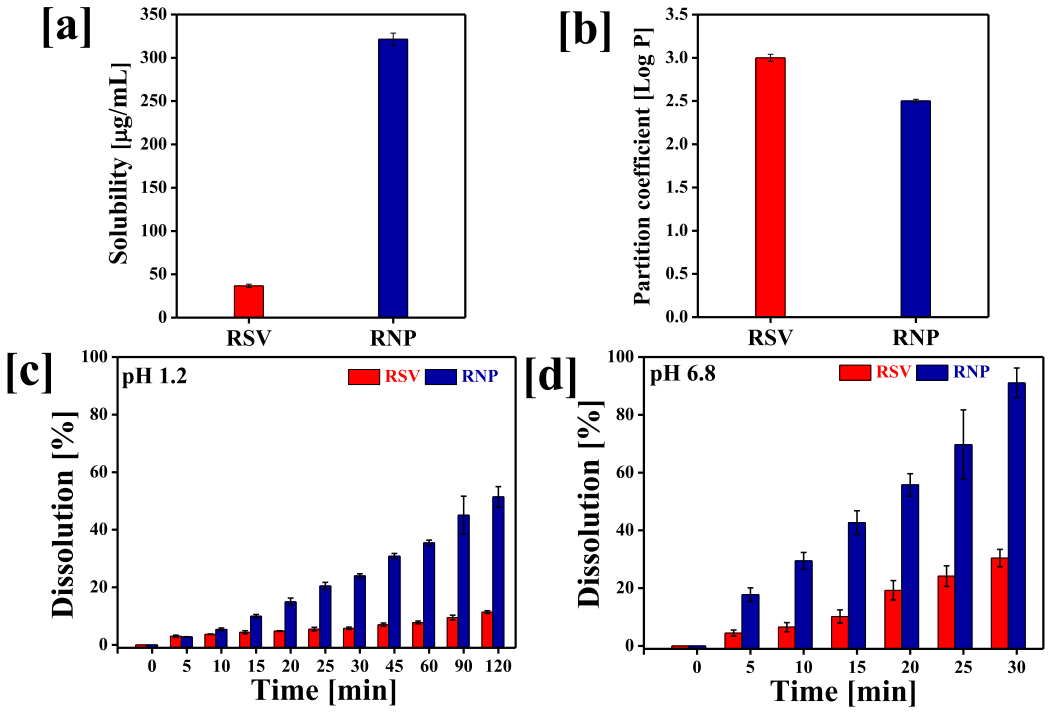

Fig. 2. (a) Solubility of RSV and RNP in water, (b) partition coefficient (Log P) of RSV and RNP; (c and d) *In vitro* dissolution of RSV and RNP in 0.1 N HCl (pH 1.2) and phosphate buffer (pH 6.8).

observed RSV content in RNP was 99.1 ± 0.4%. Therefore, it can be concluded that the prepared surfactant-free RNP formulation was stable at refrigeration conditions.

3.3. In vitro cytotoxicity study of RNP against human colorectal cancer cells

Fig. 3**a-b** showed the *in vitro* cytotoxicity of RSV and RNP against HCT 116 cancer cells The half-maximal inhibitory concentrations (IC_{50}) of RSV and RNP were found to be 37.2 ± 1.2 µg/mL and 32.6 ± 0.8 µg/

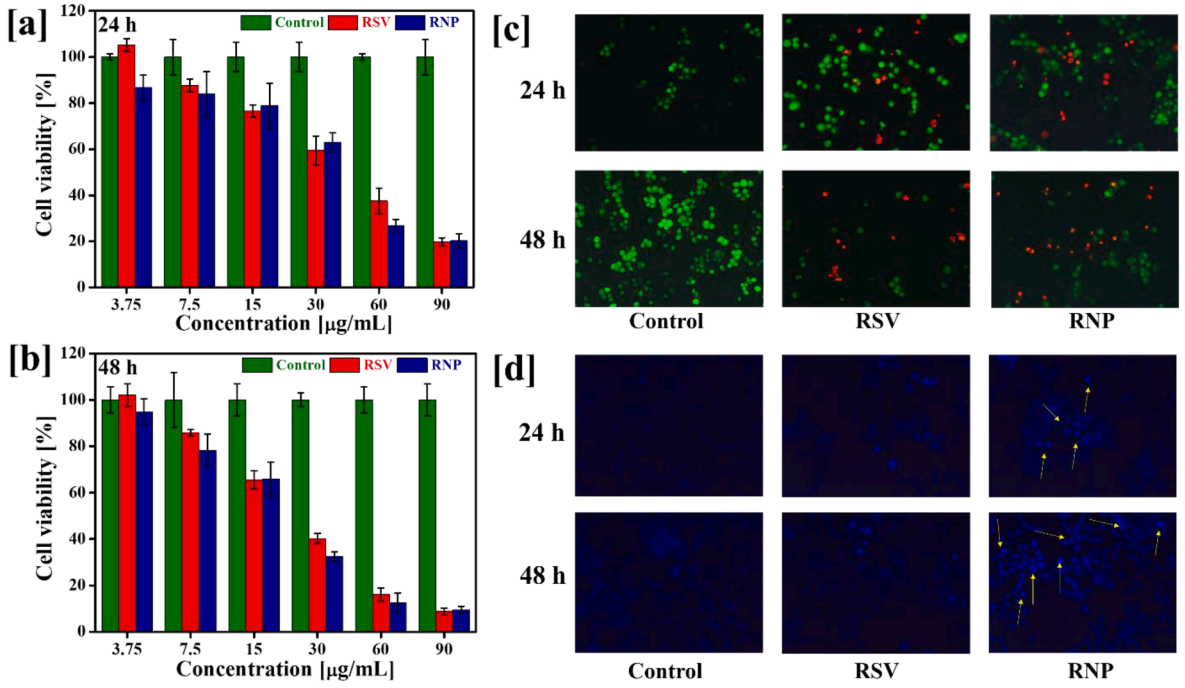

Fig. 3. (a and b) Cytotoxicity of RSV and RNP against HCT 116 colorectal cancer cell lines at 24 h and 48 h, respectively, (c) Acridine orange-ethidium bromide staining of HCT 116 colorectal cancer cell lines after exposure of RSV and RNP, and (d) Hoechst 33,342 staining for the detection of apoptotic nuclei of HCT 116 colorectal cancer cells after incubation with RSV and RNP. (For interpretation of the references to colour in this figure legend, the reader is referred to the web version of this article.)

mL after 24 of incubation, respectively. The IC_{50} values were decreased to 23.5 ± 2.8 μg/mL for RSV and to 19.7 ± 3.5 μg/mL for RNP after 48 h (Fig. S1). Fig. 3**c** shows the AO/EB staining assay, as the time of incubation was increased, the number of necrotic cells was increased while the number of live cells (with green fluorescence) was decreased. It was found that the induction of apoptosis was more in RNP-treated cells than RSV-treated cells. Fig. 3**d**, the bright nuclei (chromatin concentration) represent the late apoptosis or necrosis cells. The results showed the HCT 116 cells treated with RNP showed more bright nuclei which further confirmed that the prepared RNP formulation was more toxic to the human colorectal HCT 116 cells than the native RSV.

3.4. Pharmacokinetic study

Fig. S2 shows the RSV plasma concentration versus time profile, and the pharmacokinetic (PK) parameters are listed in Table S4. The AUC of the RNP (2.32 ± 0.28 μg/ml × h) was 2.36 times significantly higher ($p < 0.0001$) than the pure RSV (0.98 ± 0.03 μg/ml × h). The plasma C_{max} was found to be 0.23 ± 0.02 μg/mL for RSV and 0.62 ± 0.09 μg/mL for RNP. The increased AUC and C_{max} values suggested the higher absorption of the RSV after administration as RNP. This demonstrated that the as-made RNP had greater anticancer activity and bioavailability as compared to pure RSV.

4. Conclusion

The RNP formulation prepared using 0.5% w/v of SDS exhibited the lowest particle size (81 nm) distribution with 0.202 PDI and −15.4 mV zeta potential values. Solid-state characterization of the amorphous RNP confirmed by the PXRD and DSC analysis and the complete removal of surfactant from the nanoparticle surface confirmed by the ^{1}H NMR and FTIR spectroscopy. The carrier-free and amorphous RNP significantly enhance the water solubility, dissolution, stability with decreasing hydrophobicity as compared to crystalline RSV. Therefore, the amorphous RNP exhibited better *in vivo* performance compared to raw RSV powder. The increase in C_{max} and AUC confirmed the increase in oral bioavailability due to enhance solubility, amorphous nature, and better dissolution profile of RSV from the RNP formulation.

CRediT authorship contribution statement

Ashok Kumar Jangid: Conceptualization, Methodology, Writing - original draft, Software. **Krunal Patel:** Investigation. **Poonam Jain:** Data curation, Software, Formal analysis. **Sunita Patel:** Validation. **Kanakaraju Medicherla:** Formal analysis. **Deep Pooja:** Writing - review & editing, Visualization. **Hitesh Kulhari:** Conceptualization, Writing - review & editing, Supervision.

Declaration of Competing Interest

The authors declare that they have no known competing financial interests or personal relationships that could have appeared to influence the work reported in this paper.

Acknowledgments

Authors thank the Central University of Gujarat, Gandhinagar for providing the necessary facilities and support. HK acknowledges the Department of Science and Technology (DST), New Delhi for an INSPIRE faculty award and SERB for ECR award. AKJ, KP, PJ acknowledge the University Grant Commission (UGC), New Delhi for Ph.D. fellowships.

Appendix A. Supplementary data

Supplementary data to this article can be found online at https://doi.org/10.1016/j.matlet.2021.130340.

References

[1] Q. Shuai, G. Zhao, X. Lian, J. Wan, B. Cen, W. Zhang, J. Liu, W. Su, H. Wang, Self-assembling poly(ethylene glycol)-block-polylactide-cabazitaxel conjugate nanoparticles for anticancer therapy with high efficacy and low *in vivo* toxicity, Int. J. Pharm. 574 (2020), 118879.
[2] S. Kalepu, V. Nekkanti, Insoluble drug delivery strategies: review of recent advances and business prospects, Acta Pharmaceutica Sinica. B. 5 (2015) 442–453.
[3] A.M. Stewart, M.E. Grass, Practical approach to modeling the impact of amorphous drug nanoparticles on the oral absorption of poorly soluble drugs, Mol. Pharm. 17 (2020) 180–189.
[4] R. Kumar, A.K. Thakur, P. Chaudhari, N. Banerjee, Particle size reduction techniques of pharmaceutical compounds for the enhancement of their dissolution rate and bioavailability, J. Pharm. Innovation (2021).
[5] C. Qiu, D. Julian McClements, Z. Jin, Y. Qin, Y. Hu, X. Xu, J. Wang, Resveratrol-loaded core-shell nanostructured delivery systems: Cyclodextrin-based metal-organic nanocapsules prepared by ionic gelation, Food Chem. 317 (2020), 126328.
[6] F. Ahmed, B. Ijaz, Z. Ahmad, N. Farooq, M.B. Sarwar, T. Husnain, Modification of miRNA Expression through plant extracts and compounds against breast cancer: Mechanism and translational significance, Phytomedicine 68 (2020), 153168.
[7] M. Correia-da-Silva, V. Rocha, C. Marques, C.M. Deus, A. Marques-Carvalho, P. J. Oliveira, A. Palmeira, M. Pinto, E. Sousa, J.M.S. Lobo, I.F. Almeida, Potential benefits of a sulfated resveratroderivative for topical application, J. Mol. Endocrinol. 61 (2018) 27–39.
[8] P. Benjasirimongkol, S. Piriyaprasarth, P. Sriamornsak, Design and optimization of resveratrol-loaded porous calcium silicate powders for dissolution and photostability enhancement, Heliyon. 5 (2019), e01399.
[9] I.C.C.M. Porto, T.G. Nascimento, J.M.S. Oliveira, P.H. Freitas, A. Haimeur, R. França, Use of polyphenols as a strategy to prevent bond degradation in the dentin–resin interface, Eur. J. Oral Sci. 126 (2018) 146–158.
[10] C. Hong, Y. Dang, G. Lin, Y. Yao, G. Li, G. Ji, H. Shen, Y. Xie, Effects of stabilizing agents on the development of myricetin nanosuspension and its characterization : An *in vitro* and *in vivo* evaluation, Int. J. Pharm. 477 (2014) 251–260.